



Systematic application of UPLC-Q-ToF-MS/MS coupled with chemometrics for the identification of natural food pigments from Davidson plum and native currant

Thomas Owen Hay^{*}, Melissa A. Fitzgerald, Joseph Robert Nastasi

School of Agriculture and Food Sustainability, University of Queensland, Brisbane, QLD, Australia

ARTICLE INFO

Keywords:

Traditional foods
Colour
Metabolomics
Anthocyanins
Chemometrics
CIELAB
UPLC-Q-ToF-MS/MS

ABSTRACT

This study investigates the potential of Australian Traditional foods as novel sources of natural colourants for food applications, employing untargeted metabolomics and chemometrics. Two native species were analysed: Davidson plum and native currant. The species were quantitatively assessed for colour properties using the CIELAB colour system in conjunction with Ultra Performance Liquid Chromatography-Quadrupole Time of Flight Tandem Mass Spectrometry (UPLC-Q-ToF-MS/MS). The results highlight diverse phenolic, flavonoid, and significant anthocyanin levels in Davidson plum and native currant, contributing to their robust red hues, comparable to commercial blueberry standards. Davidson plum and native currant exhibited high phenolic, flavonoid, and anthocyanin levels, contributing to vibrant red hues and significant bioactivity. Compared to blueberry, these species showed greater redness (a^*) and chroma. Native currant demonstrated the highest phenolic content (146.73 mg g^{-1}), anthocyanin content (14.48 mg g^{-1}), and antioxidant activity ($95.48 \text{ } \mu\text{mol Trolox equivalents/g}$). The chemometric analysis identified 46 key pigment metabolites, including anthocyanins and flavonoids, directly correlating to observed colour properties. UPLC-Q-ToF-MS/MS combined with CIELAB colourimetry facilitated pigment identification and colour analysis. These findings position Davidson plum and native currant as promising natural food colourants and functional ingredients. Additionally, the study underscores the efficacy of integrating chemometric analysis with CIELAB and UPLC-Q-ToF-MS/MS methodologies for pinpointing specific metabolites that influence the colour properties of these Traditional foods. This approach facilitates a deeper understanding of how indigenous Australian bushfoods can be innovatively incorporated into the food industry, aligning with consumer demand for natural and sustainable food options.

1. Introduction

The inherent visual appeal of food has long captivated human senses, with colour playing a pivotal role in arousing appetite and shaping our culinary experience (Manzoor et al., 2021). Recently, growing concerns over artificial additives and their health connotations are driving consumer demand for clean-label products (Ahmed et al., 2021; Bora et al., 2019). Within the food industry, a major focal point is the replacement of synthetic colourants with naturally sourced colourings (Echegaray et al., 2023). The biodiscovery of novel colourants spans scientific, regulatory, and industry sectors with the common goal of discovering and utilising robust colours that meet food safety standards and consumer expectations.

Presently, natural sources of colour for use in food production come

from a wide variety of plant metabolites, including chlorophylls for greens, curcuminoids or carotenoids for oranges and yellows, and anthocyanins for reds and purples (Bora et al., 2019). The inclusion of plant metabolites also has secondary benefits for food formulations. Food metabolites can also exhibit preservative effects such as antifungal (Redondo-Blanco et al., 2020), antimicrobial (Batiha et al., 2021), and antioxidative (Mani et al., 2020). Moreover, current scientific literature supports that health is improved by the dietary inclusion of bioactive secondary metabolites (Deledda et al., 2021; Gantenbein & Kanaka-Gantenbein, 2021; Papas, 2019). As a result, increasing consumer demand for health-conscious and environmentally friendly products has been driving advances in natural pigment research (Ding et al., 2024). Research is largely focused on novel pigment production methods (Lyu et al., 2022), characterisation and stabilisation methods (Ding et al.,

^{*} Corresponding author.

E-mail address: t.hay@uq.edu.au (T.O. Hay).

<https://doi.org/10.1016/j.fochx.2024.102072>

Received 28 July 2024; Received in revised form 21 November 2024; Accepted 4 December 2024

Available online 7 December 2024

2590-1575/© 2024 Published by Elsevier Ltd. This is an open access article under the CC BY-NC-ND license (<http://creativecommons.org/licenses/by-nc-nd/4.0/>).

2024), and the exploration of novel pigment sources (Hay et al., 2022; Nwoba et al., 2020).

Traditional foods are integral to the cultural heritage and practices of specific communities or regions. These foods are typically derived from local, natural ingredients and have been prepared and consumed over generations using Traditional methods (Lim et al., 2020). Traditional foods are increasingly recognised as a novel source of valuable metabolites (Hay et al., 2022; Lim et al., 2020). Australian Traditional foods or 'bushfoods' present a unique blend of novelty and cultural attenuation, rooted in Indigenous Knowledge and contemporary culinary experimentation. Current literature has affirmed that Australian Traditional foods are an exceptional source of bioactive compounds (Lim et al., 2020; Mani et al., 2020; Nastasi, Daygon, et al., 2023; Njume et al., 2020). However, investigations that focus on the food colouring potential of Australian Traditional foods are currently minimal (Hay et al., 2022). Therefore, the opportunity to investigate Australian Traditional foods for novel pigment sources is greatly apparent. The outcome of such work can be beneficial to both consumers, as well as a valuable addition to the Australian Traditional foods sector.

Recent collaborations with Indigenous custodians enabled the investigation of various fruits with colourant potential, many of which have not been analysed previously. The present work focused on two Traditional food species suggested for novel pigment sources. These include the Davidson plum (*Davidsonia puriens*), an astringent dark red plum with bright red flesh that has previously been analysed for its composition (Chuen et al., 2016), and the native currant (*Antidesma erostre*), a small, dark purple berry, which has received minimal pigment investigation. The selection criteria of the Davidson plum and native currant were made based on early observations from a wide range of Traditional food samples. Both fruits possess a dark purple skin with a red to purple flesh, indicating the presence of anthocyanins or betalains. There is a wide range of fruit and vegetables that are utilised as natural sources of red to purple pigments, including beetroot (Mudgal et al., 2022), red cabbage (Zanoni et al., 2020), and blueberry (da Rosa et al., 2019; Darniadi et al., 2018). It is necessary to compare colour extracts of Traditional foods to such species to position native fruits within an industry-relevant context to gain insight into their relative value to the colourant industry. Blueberry was selected as a comparison sample in this study due to its established role as a benchmark for natural food colourants (Yang et al., 2022). Its high content of anthocyanins, which are well-documented for their blue to red pigmentation, makes it a relevant standard for evaluating the colourimetric and metabolomic properties of potential alternative pigment sources.

The structural identification of plant pigments has undergone significant advancements due to the development of sophisticated analytical techniques. Plant pigments including anthocyanins, flavonoids, carotenoids, betalains, and chlorophylls, are highly diverse compounds, and elucidating their presence and contents requires highly specified methodologies. The more conventional methods such as Ultraviolet-visible spectrophotometry can be well-suited to quantifying such compounds due to their absorbance at known wavelengths (Lee et al., 2005). Technologies such as Ultra-Performance Liquid Chromatography coupled with Quadrupole Time-of-Flight Mass Spectrometry (UPLC-Q-ToF-MS/MS), Nuclear Magnetic Resonance (NMR), and Thin-Layer Chromatography (TLC)-Raman spectroscopy have been pivotal in characterising these pigments at a molecular level (Li et al., 2021; Lim et al., 2020; Yan et al., 2023). For instance, UPLC-Q-ToF-MS/MS offers high sensitivity and resolution, enabling the detailed annotation of pigment metabolites, including their glycosidic linkages and derivative forms (Escher et al., 2020). A practical method of colour analysis in food is the CIELAB colour system (Luo, 2023). The CIELAB technique evaluates food colour objectively by applying an empirical value for colour coordinates in a 3D space and is crucial for quality control and determining consumer appeal (Spence et al., 2022). However, each method comes with limitations. UPLC-Q-ToF-MS/MS, while powerful, is subject to intensive feature annotation based on library matching, or the use of

in silico modelling to identify a target feature. Such annotations can be ambiguous where rigorous methodology is not implemented. Moreover, given that plant pigments are structurally diverse and often exist in conjugated forms, their comprehensive identification is complex. Furthermore, their stability is influenced by environmental factors such as pH, temperature, and light exposure, complicating the standardisation of both extraction and analysis (Manzoor et al., 2021). For example, anthocyanins are highly sensitive to pH changes, which can lead to pigment degradation or structural transformation during extraction and processing (Trouillas et al., 2016). These challenges underscore the need for continuous refinement of analytical workflows and the development of cost-effective, high-throughput methods for pigment characterisation.

Many species of Traditional foods lack compositional analysis of their secondary metabolites. Therefore, if Traditional food samples have colour potential, it is desirable to establish the compositional variation to existing industry standards like blueberry and to correlate their compositional variation to their colour perception. Presently, there is limited literature that couples UPLC-Q-ToF-MS/MS with CIELAB colourimetry for understanding how the metabolic composition of a sample influences the perceived colour. UPLC-Q-ToF-MS/MS enables precise identification and quantification of colour-contributing metabolites, detailing their structural diversity and abundance. When paired with CIELAB metrics, which objectively quantify colour attributes like lightness (L^*), redness (a^*), and yellowness (b^*), this approach could allow for the direct correlation of specific metabolites to observed colour properties. This integration can reveal the pigmented compounds responsible for the perceived colour and facilitate the optimisation of pigment profiles for food and nutraceutical applications. As such, the present study will determine the metabolomic profile, antioxidant activity, and CIELAB colour metrics of two Traditional Foods compared to blueberry. The study will also produce a stepwise workflow for employing multivariate modelling to correlate the metabolomic profile of a food sample to its perceived colour.

2. Materials and methods

2.1. Materials and reagents

The plant materials were collected from Sevgen Farm (*Davidsonia puriens*) at $-26.44710, 152.88974$ and Witjuti grub Farm (*Antidesma erostre*) at $-26.64148, 152.81429$. The identity of the samples was confirmed by a botanist at the University of Queensland as a second point of species identification. *Davidsonia puriens* trees range in age from 5 to 10 years. *Antidesma erostre* plant age was approximately 2 to 3 years. Davidson plum fruit maturity was established as fruit having a dark red skin colour and a total soluble solids content of 13–15%. *Antidesma* fruit was selected as ripe based on colour and taste by Witjuti grub farm horticulturalists. All chemicals used were analytical grade. The organic solvents and materials were supplied by Sigma Aldrich (St. Louis, MO, USA) and reagents were prepared freshly on the day of analysis.

2.2. Extraction protocol

All plant samples were received fresh and stored on ice or frozen by producers. The growers determined fruit ripeness via an in-house quality assurance protocol based on a colour scale and the total soluble solids. All colour extracts were made using the peel and pulp. Samples were frozen to -80°C and dried for 72 h in a Christ alpha 1–2 LD freeze drier (Martin Christ, Osterode, Germany) at 1.0 mPa. The freeze-dried sample matter was immersed in liquid nitrogen before grinding in a Tissuelyser II ball and socket mill (Qiagen, Tokyo, Japan) at $30 \times 1/\text{s}$ Hz for 30 s and then sieved through a $50 \mu\text{m}$ mesh. Each plant sample was extracted in triplicate (1 g), and each replicate was twice extracted sequentially in 10 mL of 80% ethanol acidified to 2 pH with 6 N HCl. Each 10 mL extraction was sonicated (Soniclean 160TD, Mektronics, Australia) for

15 min at 100 Hz, vortexed for 30 min in the dark, and incubated at 4 °C for 2 h. Next, the supernatants were combined and centrifuged (Thermo Fischer Scientific, Waltham, MA, USA) at 4500g for 15 min, and the pooled supernatant was filtered using Wattman filter paper strip (item number: 1001 110). The final extract concentrations tested were 50 mg mL⁻¹. The ethanol extracts were then stored at -80 °C until testing.

2.3. Colour measurement

Colour analysis was adapted from the method by [Nastasi, Fitzgerald, and Kontogiorgos \(2023\)](#) with changes. The colour coordinates L*, a*, and b* was measured using an FRU Precise Colour Reader (ShenZhen Wave Optoelectronics Technology Co., Ltd.). The colourimeter was calibrated using a white reference plate, and an 8 mm adapter was attached to the colourimeter for sample measurement. For analysis, ethanol extracts were poured to fill a 35 × 10 mm cell culture dish (Corning Incorporated, Corning, NY, USA). Illumination was provided from two 63 LED light bars (12,000–13,000 LM) and samples were photographed using a smartphone camera in a 45 cm³ photo box. The Hue angle (°) and Chroma (%) were calculated by eq. (1) and (2) respectively:

$$\text{Hue} = \tan^{-1} \left(\frac{b^*}{a^*} \right) \quad (1)$$

$$\text{Chroma} = \sqrt{a^{*2} + b^{*2}} \quad (2)$$

2.4. Quantification of phenolic classes

2.4.1. Total phenolic content (TPC)

Metabolite classes of phenolic acids, flavonoids and anthocyanins were quantified according to established methods with modifications ([Lee et al., 2005](#); [Nastasi, Fitzgerald, & Kontogiorgos, 2023](#); [Sánchez-Rangel et al., 2013](#)). The ethanolic extracts were mixed with a 0.2 N Folin-Ciocalteu reagent and incubated at room temperature for 3 min. Next, 7.5 % w/v sodium carbonate was mixed into the sample and incubated for 2 h in the dark, and the absorbance was measured at 765 nm with a Floustar optima microplate reader (BMG Labtech, Victoria, Australia). Gallic acid stock solution (1 mM) in distilled water was used to generate an 8-point calibration curve (0–120 μM). The blank consisted of Folin-Ciocalteu reagent and sodium carbonate.

2.4.2. Total flavonoid content (TFC)

The extracts and standards were mixed with 5 % w/v sodium nitrite and incubated at room temperature for 5 min. Following that step, 2 % w/v aluminium chloride was added, mixed, and incubated for a further 6 min at room temperature. Finally, 1 M sodium hydroxide was added, mixed, and incubated for 10 min at room temperature before being read spectrophotometrically at 510 nm (Floustar optima microplate reader, BMG Labtech, Victoria, Australia). A stock solution of 1 mM quercetin dissolved in ethanol was used to generate individual standards for a 7-point calibration curve (10–80 μM).

2.4.3. Total monomeric anthocyanin content (TMAC)

The total monomeric anthocyanin content (TMAC) of the plant extracts was determined according to the AOAC method 2005.02 ([Lee et al., 2005](#)). In brief, each extract was diluted with 0.025 M potassium chloride buffer (pH 1) and measured on a spectrophotometer (Shimadzu UV1800, Shimadzu, Kyoto, Japan) at 520 nm and 700 nm. This process was repeated with a 0.4 M sodium acetate buffer (pH 4.5). The blank consisted of an 80 % ethanol and 20 % distilled water solution, and anthocyanin concentration was expressed as cyanidin-3-glucoside equivalents.

2.5. Antioxidant activity

The scavenging activity of the antioxidant content was determined by the DPPH (2,2-diphenylpicrylhydrazyl) assay following [Chuen et al. \(2016\)](#) with modification. In brief, each extract was mixed with 100 μM DPPH solution and measured at 520 nm using a Floustar optima microplate reader (BMG Labtech, Victoria, Australia). Samples were kept in the dark and measured at 10 min intervals for 40 min. A stock solution of 100 μM Trolox dissolved in ethanol was used to generate individual standards for a 7-point calibration curve (5–40 μM). Assay results of the 40 min measurement are reported as μmol Trolox equivalents per gram dry weight.

2.6. Metabolomic profiling of blueberry, native currant, and davidson plum

The Ultra Performance Liquid Chromatography-Quadrupole Time of Flight Tandem Mass Spectrometry (UPLC-Q-ToF-MS/MS) analysis was performed using a Shimadzu Nexera UHPLC system (Kyoto, Japan; LC-30 CE pump, SIL-30 AC autosampler and CTO-30 A column oven) equipped with a Shimadzu Q-TOFMS-9030 detector. The separation of the sample analytes was conducted on a Restek Biphenyl, 2.7 μm (100 × 2.1 mm Column, Product Code: 9309A12, Restek, Saunderton, England). The mobile phase consisted of A (0.05 % [v/v] formic acid, and B (0.05 % [v/v] formic acid in methanol). The sample injection volume was 1 μL with a consistent flow rate of 0.4 mL/min. The gradient program was as follows: 0 % B for 0–1.5 min, 5 % B for 1.5–2.5 min, 10 % B for 2.5–4.5 min, 30 % B for 4.5–8 min, 40 % B for 8.0–12.0 min, 60 % B for 12.0–13.0 min, 80 % B for 13.0–14.0 min, 100 % B for 14.0–15.0 min, 100 % B for 15.5–16.0 min, 0 % B for 16.0–17.0 min. The column temperature and autosampler were set at 40 °C. Ionisation for positive and negative modes was assessed. The mass spectrometer was operated using an electrospray ionisation (ESI) source with collision energy set at 70 eV, the fragmentor voltage was 100 V. The settings were: Data independent acquisition, nebulizing gas flow of 3.0 L/min, Drying and heating gas flow was 10.0 L/min. The nebulizer pressure was 230 kPa. The source temperature was 120 °C, and the desolvation temperature was 200 °C.

2.7. Processing of LC-MS/MS data

Data files were extracted from the Shimadzu Lab Solutions Software (Shimadzu, Kyoto, Japan) in the MzML format. Next, the MzML files were imported to MS-DIAL v4.80 to process the positive and negative ionisation mode datasets. All samples were aligned using a mixed QC file, and the alignment file was normalised by the total ion chromatogram method. Features were reference-matched with MS Dial using positive and negative mode libraries with a match threshold of >85 %. The reference-matched compounds were each annotated using their MS2 spectral matching and cross-referenced to their MS Finder score. Compounds fragmented in positive and negative ionisation modes were resolved based on their highest abundance across the sample groups. The peak list was exported to Microsoft Excel for import into statistical software.

2.8. Statistical analysis

Univariate analysis was performed using GraphPad Prism version 9.4.1 for Windows (GraphPad Software, San Diego, California USA, www.graphpad.com). One-way ANOVA and Fisher LSD post-hoc analysis were conducted to a confidence of $p < 0.05$. Chemometric analysis of the metabolite data in each extract was performed using SIMCA 18 (Umetrics, Sweden). Principal Component Analysis (PCA) models were generated using the putatively annotated peak list exported from MS-Dial. Cross Validation (CV) for model calibration was performed using SIMCA 18 standard protocol ($G = 7$, leave one out). The confidence level for all analyses was 95 %. PCs generated for the PCA were

considered significant if they met the criteria for Rule (R1) as determined by SIMCA 18 protocols. Using the autofit option for model calibration, the appropriate number of PCs was chosen for the deconvolution of the data sets. The Q^2 value is determined by the function $Q^2 = 1 - \text{PRESS}/\text{SS}$ where $\text{PRESS} = \sum (\text{observed} - \text{predicted})^2$ and SS is the sum of squared deviations from the mean of X. Q^2 can be used to support the predictiveness of a component and Q^2 close to that of R^2 indicates good predictability. The PLS and PLS-DA models used Pareto scaling, and the coefficients were scaled and centred.

3. Results and discussion

3.1. Visual colour of traditional foods

Firstly, the species were freeze-dried and extracted using acidified 80 % ethanol. It has been shown that the optimisation of pigment extraction is highly variable depending on the ontologies of targeted metabolites being extracted. Therefore, acidified ethanol was used given its food safety and generally high extraction of polar compound groups including betalains, flavonoids and anthocyanins (Li et al., 2021). Moreover, the extraction methodology was simplified to accommodate the limitations of processing by small to medium enterprises within the food industry. The ethanolic extracts of freeze-dried whole fruit were made at a consistent concentration (50 mg mL⁻¹) and were photographed under consistent light conditions (12,000–13,000 LM LED lamp) and depth (10 mm) to enable comparative analysis at the same conditions.

Fig. 1 shows each of the Traditional foods and their respective extracts. The extraction of blueberry pigments has been covered extensively in literature and is an industry standard for a natural colourant sourced from a berry (Faria et al., 2005; Li et al., 2021; Yan et al., 2023). As such, blueberry (*Vaccinium corymbosum*) was used as an extract comparison in all analyses. The visual description of the Davidson plum was comparable to the blueberry though slightly lighter. The native currant was also a burgundy-red colour like the blueberry and Davidson plum extracts.

3.2. CIELAB colourimetry

Next, CIELAB colourimetry was used to for the numerical interpretation of the extracts within a three-dimensional colour space. The

CIELAB data obtained by colourimetric analysis of the Traditional foods and blueberries are reported in Table 1. The lightness (L^*) ranged from 23.54 in the native currant to 39.28 in the blueberry. The lightness of native currant and Davidson plum significantly ($p < 0.05$) to the blueberry. The red a^* ranged from 2.17 in the blueberry to 25.07 in the Davidson plum. The blueberry a^* was dissimilar to the Davidson plum and native currant extracts at 20.44 and 25.07, respectively. The b^* measuring the blue to yellow space ranged from -1.89 in the blueberry to 8.78 in the Davidson plum. The hue angle ranged from 16.30° in the native currant to 354.64° in the blueberry. The Davidson plum (19.30°) and native currant (16.30°) were closely related in hue angle, falling into a red quadrant, with blueberry slightly separated into a magenta-to-red quadrant. The chroma percentage (otherwise considered the saturation) was significantly different between the blueberry (20.26 %), Davidson plum (26.56 %) and the native currant (21.30 %).

The translation of colour from fresh, whole fruit to extracts is highly variable and subject to extraction processes. Previously, a comprehensive analysis of blueberries from 20 cultivars by Yan et al. (2023) determined the CIELAB of the skin surface. Elsewhere, blueberry liquor colour was assessed by Caldeira et al. (2018) where the colour of the beverages was influenced by the sweetener used, specifically the amber colour of honey. In each case, CIELAB methodology was employed, and the differences between reported data for the same fruit exemplify the limitations of colourant extract comparison between differing

Table 1

Colour metrics of blueberry, davidson plum, and native currant.

Sample	Scientific name	L^*	a^*	b^*	Hue (°)	Chroma (%)
Blueberry	<i>Vaccinium corymbosum</i>	39.28	2.17	-1.89	354.64	20.26 ± 0.01 ^a
		± 0.11 ^a	± 0.02 ^a	± 0.01 ^a	± 0.28 ^a	
Davidson plum	<i>Davidsonia puriens</i>	26.12	25.07	8.78	19.30	26.56 ± 0.38 ^b
		± 0.34 ^b	± 0.31 ^b	± 0.07 ^b	± 0.36 ^b	
Native currant	<i>Antidesma erosre</i>	23.54	20.44	5.98	16.30	21.30 ± 0.24 ^c
		± 0.54 ^c	± 0.14 ^c	± 0.37 ^c	± 0.87 ^c	

CIELAB colorimetric values, Hue angle and chroma % of Traditional foods and blueberry (n = 3). Different letter superscripts in the same column indicate a statistically significant difference ($P < 0.05$) using the post-hoc Tukey test.



Fig. 1. Blueberry (*Vaccinium corymbosum*), davidson plum (*Davidsonia puriens*), and native currant (*Antidesma erosre*). The native currant shows a range of colours during ripening, from yellow to black. Ripened fruits were used for colour extracts. (For interpretation of the references to colour in this figure legend, the reader is referred to the web version of this article.)

processing and imaging conditions. A similar extraction protocol to the present study using acidified ethanol was employed by Cesa et al. (2017), and most closely resembles the blueberry CIELAB results in Table 1. The native currant and Davidson plum samples were shown to have a similar lightness (L^*), and blue-to-yellow (b^*) coordinates to that of blueberry extract at the same concentration (Table 1). However, the green to red (a^*) range was 10-fold higher for the two native extracts, suggesting a closer association with redness than the blueberry. This correlated with the imaging for the native currant sample the most, which appeared darker than the blueberry and Davidson plum extracts. The Davidson plum and native currant samples could be considered for natural colourant applications. However, the analysis was expanded to show what metabolic components contribute to their colouration. Moreover, bioactive components are a large advantage to the use of natural colourants, and identifying their constituent can increase their value as a food additive.

3.3. Quantified phenolic classes and antioxidant activity

Quantitative benchtop analysis of the phenolic, flavonoid, and anthocyanin contents was conducted to elucidate the compound groups present in the Traditional foods with strong pigmentation (Table 2). The total phenolic content was measured as gallic acid equivalence (mg g^{-1} dry weight). Total phenolic content was significantly highest in the native currant ($146.73 \pm 4.35 \text{ mg g}^{-1}$), followed by blueberry ($89.03 \pm 3.65 \text{ mg g}^{-1}$). The Davidson plum had a moderate content and showed no significant difference ($p < 0.05$). The total flavonoid content was measured by quercetin equivalence (mg g^{-1} dry weight). Davidson plum and native currant were similar in flavonoid content, with no significant difference between the blueberry, Davidson plum and native currant ($p < 0.05$).

Total anthocyanin content was measured via the pH differential method and reported as cyanidin-3-glycoside equivalence. A significantly higher content was found in the native currant ($14.48 \pm 2.85 \text{ mg g}^{-1}$) above Davidson plum ($8.06 \pm 1.66 \text{ mg g}^{-1}$), which was significantly higher than blueberry ($7.16 \pm 0.08 \text{ mg g}^{-1}$). The scavenging activity of the antioxidant content was measured via the DPPH method (Chuen et al., 2016) and reported as $\mu\text{mol Trolox equivalents (TRE)}$. The significantly highest extract was native currant ($95.48 \pm 2.57 \mu\text{mol TRE g}^{-1}$). Davidson plum ($18.66 \pm 1.37 \mu\text{mol TRE g}^{-1}$) was next highest and significantly greater than blueberry ($14.45 \pm 0.17 \mu\text{mol TRE g}^{-1}$).

Blueberry was shown to be high in polyphenols, flavonoids, and anthocyanins, which matched previously reported phenolics data (Faria et al., 2005) while flavonoid and anthocyanin content fell within the lower range previously reported (Yan et al., 2023). Quantitative assessment of phenolic acids and flavonoids can be expected to vary due to genotype, seasonality, and geographic differences when growing. The

Table 2

Polyphenol content and antioxidant activity of blueberry, davidson plum, and native currant.

Sample	Total Phenolics (mg GAE/g DW)	Total Flavonoids (mg QUE/g DW)	Total anthocyanins (mg CGA/g DW)	DPPH ($\mu\text{mol TRE/g DW}$)
Blueberry	89.03 ± 3.65^a	99.19 ± 4.16^a	7.16 ± 0.08^a	14.45 ± 0.17^a
Davidson plum	28.32 ± 3.24^b	48.56 ± 2.52^b	8.06 ± 1.66^b	18.66 ± 1.37^b
Native currant	146.73 ± 4.35^c	42.73 ± 2.63^b	14.48 ± 2.85^c	95.48 ± 2.57^c

The values are the means \pm standard deviations for triplicate extracts. GAE = gallic acid equivalents. QUE = quercetin equivalents. CGA = cyanidin-3-glycoside equivalents. TRE = Trolox equivalents. DW = dry weight. Different letter superscripts in the same column indicate a statistically significant difference ($P < 0.05$) using the post-hoc Tukey test.

total phenolic and total anthocyanin contents were especially high in the native currant extract. *Antidesma erosre* has recently gained research interest (Dechayont et al., 2017; Krongyut & Sutthanut, 2019; Puangpoy et al., 2024), however, such previous investigations are largely focused on *Antidesma bunuis* and its leaf content. The previously reported phenolic content of *A. bunuis* and *A. parvifolium* is consistent with the current analysis of *Antidesma erosre*, while the antioxidant scavenging activity was 10-fold higher in *Antidesma erosre* than previous values for *A. bunuis* (Krongyut & Sutthanut, 2019; Tan et al., 2011). To our knowledge, the flavonoid and anthocyanin content has not been reported for *A. erosre*. The results shown here indicate that *A. erosre* is highly valuable as a colourant and nutraceutical ingredient. The total phenolic and anthocyanin contents of Davidson plum were consistent with previously reported values (Nirmal et al., 2021). Davidson plum has received greater focus in the literature compared to native currant.

The combination of CIELAB colourimetry and bioactive data demonstrated the value of the native currant and Davidson plum. Each species possesses a novel content of bioactive compounds that were either comparable to or exceeded blueberry, though were slightly differentiated in terms of colour as interpreted via CIELAB colourimetry. Such differentiation was expected to be a result of composition and a synergistic 'entourage' effect of the colour-contributing ontologies within the phenolic, flavonoid and anthocyanin classes (de Araújo et al., 2021). Given the health benefits of dietary inclusion of phenolic compounds (Di Lorenzo et al., 2021; Rana et al., 2022), the elucidation of specific compounds that contribute to the two Traditional food species poses a higher level of evaluating their industrial potential. To this end, coupling mass spectrometry techniques with CIELAB metrics allowed for a chemometric approach to appraising natural colourants. The study therefore continued the comparison of native currant and Davidson plum to blueberry extract to identify the metabolic constituents of each species and contrast with their CIELAB metrics.

3.4. Stepwise chemometric analysis for colour metabolite determination in native currant, davidson plum, and blueberry

PCA of the untargeted metabolomic data was performed to assess Davidson plum and native currant similarity to blueberry (Fig. 2). Fig. 2a shows that the three species were different in feature composition via PCA, as they separated along PC1 and PC2. There were 673 shared features identified to have reference-matched MS2 fragmentation. However, feature annotation revealed that 306 of the original 673 features could be putatively matched using their MS2 spectra using MS Dial, and systematic In silico fragment matching using MS Finder software. Final cross-referencing was performed using the PubChem CID records. The PCA model in Fig. 2a explained 81.8 % of the variance across 3 components. PC1 explains 38.9 % of the total variance and shows the separation of native currant and Davidson plum from blueberry. PC2 explained a further 27.3 % of the variance and separated Davidson plum and native currant in the positive and negative directions respectively, showing further differentiation between the blueberry extract and the two Traditional food samples. PC3 did not provide further information to explain the separation of the three samples as it only explained a further 15.6 % of the total model variation. The metabolite dissimilarity between the three species is expected and consistent with our analysis. The focus of the study was to assess the native currant and Davidson plum for use as natural colourant sources. As such, the metabolites of interest to the study are only those that contribute to the colouration of the fruits. Therefore, subsequent data curation was conducted to limit the features to pigmented metabolites (Fig. 2b). The full 306 metabolites dataset was then trimmed to only the colour-contributing ontologies. After a high level of scrutiny which combined glycosidic features where sugar moieties had common mass (E.g. glucose and galactose), there were 46 shared compounds after data trimming. The compounds included one anthocyanidin, one flavanone, nine Anthocyanidin glycosides, 22 flavonoid glycosides, three

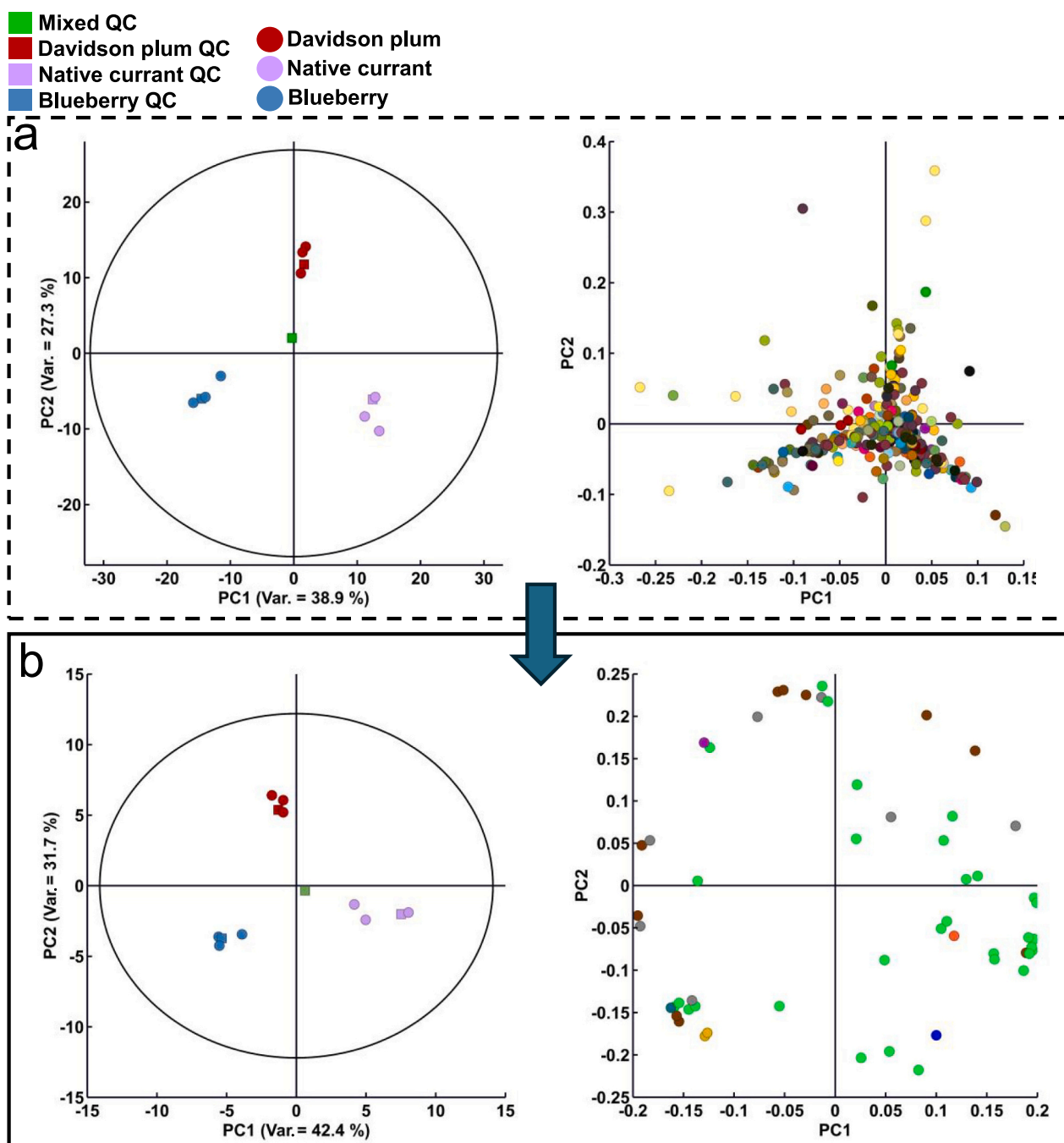


Fig. 2. Metabolites of native currant, davidson plum, and blueberry. Stepwise multivariate analysis shows trimming the dataset to only include pigment compounds as having no impact on class groupings. QC = quality control, where a mixture of the replicates was injected. Mixed QC is a mix of all samples included in the analysis. Centred mixed QC represents a good model fit for shared features. **Fig. 2a:** PCA scores and loadings plots of total metabolomic features ($n = 306$); R^2 (cum) = 81.8 % (PC1 = 38.9 %, PC2 = 27.3 %, PC3 = 15.6 %) Q^2 (cum) = 75.7 %. **Fig. 2b:** PCA scores and loadings plot using pigment metabolomic data ($n = 54$); R^2 (cum) = 87.5 % (PC1 = 42.4 %, PC2 = 31.7 %, PC3 = 13.4 %) Q^2 (cum) = 75.7 %.

flavonoids, six flavanols, and four phenolic glycosides. PCA analysis was again conducted using only these 46 compounds (Fig. 2b) which again showed the same distinct class groupings and significant differences between the three samples. This confirmed that the colour compounds used for the generation of Fig. 2b were integral to their original separation observed in Fig. 2a. The PCA model built using only the colour-contributing ontologies (Fig. 2b) explained 87.5 % of the total variance. PC1 explained 42.4 %, again showing blueberry separating from native currant and Davidson plum. PC2 explained 31.7 % of the variance and reflected the same separation as in the total metabolomic profile as demonstrated by the PCA in Fig. 2a. PC3 again provided a minimal

explanation of variance with 13.4 %. Therefore, unsupervised analysis of only the pigment compounds was as representative of the differences as when comparing the full metabolome of the samples. Therefore, subsequent analysis based on only the 46 pigment compounds, and their impact on the CIELAB metrics is validated. The 46 colour compounds used in Fig. 2b are reported in Table 3 according to best practices set by (Alseikh et al., 2021).

Table 3
Major anthocyanin and flavonoids with colour contribution in davidson plum, native currant and blueberry.

RT (Min)	Adduct	Putative metabolite name	Ontology	Molecular formula	ES Theoretical m/z	ES found m/z	m/z error (ppm)	MS/MS ES (+)/(-) Fragments	Reference CID
5.50	[M + H] ⁺	Apigenin-6-C-glucoside-7-O-glucoside	Flavonoid-7-O-glycosides	C ₂₁ H ₂₀ O ₁₀	595.165	595.167	3.36	595.167, 415.102, 313.071	162,350
4.32	[M + H] ⁺	Apigenin-7-O-glucoside	Flavonoid-7-O-glycosides	C ₂₁ H ₂₀ O ₁₀	433.112	433.114	4.62	433.114, 271.061, 123.045	5,280,704
6.76	[M-H] ⁻	Apigenin-7-O-neohesperidoside	Flavonoid-7-O-glycosides	C ₂₇ H ₃₀ O ₁₄	577.156	577.159	5.2	577.158, 269.045, 126.904	5,320,887
6.83	[M-H] ⁻	Apigetrin	Flavonoid-7-O-glycosides	C ₂₁ H ₂₀ O ₁₀	431.098	431.100	4.64	431.099, 268.038, 176.009	5,280,704
8.77	[M + H] ⁺	Calycosin-7-O-glucoside	Flavonoid-7-O-glycosides	C ₂₂ H ₂₂ O ₁₀	447.129	447.129	0.01	447.129, 285.076, 149.022	5,317,518
4.49	[M + Na] ⁺	Coniferin	Phenolic glycosides	C ₁₆ H ₂₂ O ₈	365.120	365.122	5.48	365.121, 202.059, 185.057	442,571
2.71	[M] ⁺	Cyanidin-3-O-arabinoside	Flavonoid-3-O-glycosides	C ₂₀ H ₁₉ O ₁₀	419.097	419.097	1.43	419.097 (M ⁺), 287.055 (M ⁺ - Ara)	91,810,602
3.26	[M-2H] ⁻	Cyanidin-3-O-glucoside	Anthocyanidin-3-O-glycosides	C ₂₁ H ₂₁ O ₁₁	447.092	447.094	5.37	447.097, 284.032, 125.023	441,667
3.87	[M] ⁺	Cyanidin-3-O-sophoroside	Anthocyanidin-3-O-glycosides	C ₂₇ H ₃₁ O ₁₆	611.163	611.160	5.24	611.163 (M ⁺), 287.054 (M ⁺ - C ₁₂ H ₂₂ O ₁₁)	11,169,452
4.27	[M] ⁺	Cyanidine-3-O-sambubioside	Anthocyanidin-3-O-glycosides	C ₂₆ H ₂₉ O ₁₅	581.154	581.149	6.81	581.154 (M ⁺), 287.054 (M ⁺ - C ₁₁ H ₂₀ O ₉)	78,302,543
3.02	[M + H] ⁺	Delphinidin	Anthocyanidins	C ₁₅ H ₁₁ O ₇	303.049	303.052	7.92	303.052 (M ⁺), 229.050 (M ⁺ - C ₄ H ₈ O ₂)	68,245
1.22	[M] ⁺	Delphinidin-3-galactoside	Anthocyanidin-3-O-glycosides	C ₂₁ H ₂₁ O ₁₂	465.102	465.103	2.15	465.102, 303.051, 257.040	442,567
3.84	[M] ⁺	Delphinidin-3-O-sambubioside	Anthocyanidin-3-O-glycosides	C ₂₆ H ₂₉ O ₁₆	597.147	597.144	4.24	597.146 (M ⁺), 303.051 (M ⁺ - C ₁₁ H ₂₀ O ₉)	74,977,035
2.67	[M + H] ⁺	Fisetin	Flavonols	C ₁₅ H ₁₀ O ₆	287.055	287.054	2.44	287.054 (M + H), 213.054 (M ⁺ - C ₅ H ₁₂), 137.024	5,281,614
5.88	[M + H] ⁺	Hirsutrin	Flavonoid-3-O-glycosides	C ₂₁ H ₂₀ O ₁₂	465.1023	465.105	5.38	465.107 (M + H), 449.217 (M ⁺ - O), 303.052	74,982,342
5.84	[M-H] ⁻	Isoquercetin	Flavonoid-3-O-glycosides	C ₂₁ H ₂₀ O ₁₂	463.086	463.083	7.34	463.090 (M-H) ⁻ , 301.035 (M-Glu)	5,280,804
6.57	[M-H] ⁻	Isorhamnetin-3-O-galactoside-6-rhamnoside	Flavonoid-3-O-glycosides	C ₂₈ H ₃₂ O ₁₆	623.161	623.164	4.81	623.164, 315.051	5,272,011
6.63	[M-H] ⁻	Isorhamnetin-3-O-glucoside	Flavonoid-3-O-glycosides	C ₂₂ H ₂₂ O ₁₂	477.106	477.104	4.09	477.105 (M-H), 314.044 (M-Glu)	5,318,645
6.56	[M + H] ⁺	isorhamnetin-3-O-rutinoside	Flavonoid-3-O-glycosides	C ₂₈ H ₃₂ O ₁₆	625.176	625.178	3.20	625.227, 479.121, 317.067	5,282,102
5.96	[M + H] ⁺	Isovitexin	Phenolic glycosides	C ₂₁ H ₂₀ O ₁₀	433.113	433.115	4.85	433.114, 283.061, 165.018	5,280,667
6.74	[M + H] ⁺	Kaempferol	Flavonols	C ₁₅ H ₁₀ O ₆	287.055	287.056	2.47	287.055 (M + H), 213.055, 165.018	5,280,863
6.75	[M-H] ⁻	Kaempferol-3-O-arabinoside	Flavonoid-3-O-glycosides	C ₂₀ H ₁₈ O ₁₀	417.082	417.083	2.40	417.083, 284.037, 151.000	5,282,103
8.03	[M-H] ⁻	Kaempferol-3-O-glucoside	Flavonoids	C ₂₁ H ₂₀ O ₁₁	593.130	593.132	3.37	593.13, 447.087, 285.039	5,282,102
7.46	[M-H] ⁻	Kaempferol-3-O-rhamnoside	Flavonoid-3-O-glycosides	C ₂₁ H ₂₀ O ₁₀	431.098	431.099	2.32	431.100, 284.032	5,282,153
6.35	[M + H] ⁺	Kaempferol-3-O-rutinoside	Flavonoid-3-O-glycosides	C ₂₇ H ₃₀ O ₁₅	593.148	593.151	5.87	593.154 (M-H), 285.041 (M-C ₁₂ H ₂₂ O ₁₀)	5,318,767
7.48	[M + H] ⁺	Laricitrin	Flavonoids	C ₁₆ H ₁₂ O ₆	347.075	347.076	2.88	347.076, 287.055, 153.018	5,281,644
5.23	[M-H] ⁻	Luteolin-8-C-glucoside	Flavonoid 8-C-glycosides	C ₂₁ H ₂₀ O ₁₁	447.093	447.094	2.24	447.094, 327.051, 133.029	5,280,637
13.06	[M] ⁺	Malvidin-3-galactoside	Anthocyanidin-3-O-glycosides	C ₂₃ H ₂₅ O ₁₂	491.1213	491.12131	0.02	493.135 (M ⁺), 331.081 (M ⁺ - Glu)	5,484,292
5.17	[M + H] ⁺	Myricetin	Flavonols	C ₁₅ H ₁₀ O ₈	319.0448	319.04483	0.09	319.044 (M + H), 245.049, 153.086	5,281,672
5.19	[M-H] ⁻	Myricetin-3-O-galactoside	Flavonoid-3-O-galactosides	C ₂₁ H ₂₀ O ₁₃	479.085	479.083	5.64	478.089 (M-H), 316.024 (M-Gal)	5,491,408
6.30	[M-H] ⁻	Myricitrin	Flavonols	C ₁₅ H ₁₀ O ₈	317.030	317.032	4.07	317.031 (M-H) ⁻ , 271.025 (M-COOH), 178.998	5,281,673
7.92	[M-H] ⁻	Naringenin	Flavanones	C ₁₅ H ₁₂ O ₅	271.061	271.061	0.00	317.031 (M-H) ⁻ , 271.025 (M-COOH), 178.998	5,281,672
6.63	[M + Na] ⁺	Nepetin-7-glucoside	Flavonoid-7-O-glycosides	C ₂₂ H ₂₂ O ₁₁	501.103	501.101	3.99	271.060, 171.017, 151.002	439,246
4.65	[M] ⁺	Pelargonidin-3-O-glucoside	Anthocyanidin-3-O-glycosides	C ₂₁ H ₂₁ O ₁₀	433.114	433.112	4.92	501.102, 339.048, 185.041	5,319,799
1.30	[M] ⁺	Petunidin 3-galactoside	Anthocyanidin-3-O-glycosides	C ₂₂ H ₂₃ O ₁₂	479.118	479.119	2.09	433.114 (M ⁺), 271.061 (M ⁺ - glu)	3,080,714

(continued on next page)

Table 3 (continued)

RT (Min)	Adduct	Putative metabolite name	Ontology	Molecular formula	ES Theoretical m/z	ES found m/z	m/z error (ppm)	MS/MS ES (+)/(-) Fragments	Reference CID
0.62	[M] ⁺	Petunidin-3-O-glucoside	Anthocyanidin-3-O-glycosides	C ₂₂ H ₂₃ O ₁₂	479.114	479.117	6.18	459.118 (M ⁺), 317.065 (M ⁺ - Glu)	14,311,149
3.22	[M + H] ⁺	Procyanidin	Flavonoid	C ₃₀ H ₂₆ O ₁₂	579.150	579.1503	0.05	479.119 (M ⁺), 317.067 (M ⁺ - Glu)	443,651
7.11	[M + H] ⁺	Quercetin	Flavonols	C ₁₅ H ₁₀ O ₇	303.049	303.049	0.01	579.150 (M ⁺ - H), 291.087 (M ⁺ - C15H14O2)	147,299
3.00	[M + H] ⁺	Quercetin-3-galactoside	Phenolic glycosides	C ₂₁ H ₂₀ O ₁₂	465.104	465.102	4.30	303.050, 257.045, 229.049	5,280,343
6.43	[M + Na] ⁺	Quercetin-3-O-Arabinopyranoside	Flavonoid-3-O-glycosides	C ₂₀ H ₁₈ O ₁₁	457.070	457.076	1.31	465.104, 303.050, 195.010	5,280,805
7.35	[M + H] ⁺	Quercetin-3-O-glucosyl-6-acetate	Flavonoid-3-O-glycosides	C ₂₃ H ₂₂ O ₁₃	507.113	507.113	0.01	457.074, 325.031, 155.031	5,280,459
5.79	[M + H] ⁺	Quercetin-3-O-rutinoside	Flavonoid-3-O-glycosides	C ₂₇ H ₃₀ O ₁₆	611.158	611.1606	2.85	503.321, 303.049, 187.059	10,654,747
6.6	[M + H] ⁺	Quercetin-3-O-xyloside	Flavonoid-3-O-glycosides	C ₂₀ H ₁₈ O ₁₁	435.092	435.092	0.01	611.164 (M ⁺ + H), 465.105 (M ⁺ - Rha), 303.052 (M ⁺ - Rha - Glu)	5,280,805
3.00	[M + H] ⁺	Quercetin-4-O-glucoside	Flavonoid glycosides	C ₂₁ H ₂₀ O ₁₂	465.105	465.1027	6.43	435.092, 303.050, 165.018	442,594
4.42	[M + Na] ⁺	Syringin	Phenolic glycosides	C ₁₇ H ₂₄ O ₉	395.133	395.131	5.06	465.105 (M ⁺ + H), 303.051 (M ⁺ - Glu), 195.010 (M ⁺ - Glu - C6H5OH)	12,442,954

CE (eV) = 35, Glu = glucose, Gal = galactose, Rha = rhamnose, Ara = Arabinose, Reference ID from PubChem CID. All compounds are tentatively matched from the MS/DIAL positive and negative databases and PubChem CID LC-MS, MS/MS records.

3.5. Predictive modelling of the colour metabolome relation to CIELAB colourimetry

To demonstrate the correlation between the colour and metabolites in each fruit, a PLS model was generated using the CIELAB colourimetry (Table 1), and the peak area of the pigment metabolites (compounds are reported in Table 3). PLS modelling aids in understanding the contribution of x-variables (colour metabolites), to explain a particular y-variable (CIELAB metric). The scores plot of the PLS model (Fig. 3a) had consistent grouping with the two earlier unsupervised analyses reported in Fig. 2 and therefore is predictive of the significant differences seen in the CIELAB metrics as influenced by the metabolites. The PLS loadings plot in Fig. 3a showed the grouping of particular compound classes (i.e. anthocyanins and flavonoids) with each fruit. A strong regression for each of the L* (R² = 0.998), a* (R² = 0.997) and b* (R² = 0.994) was observed (Q² (cum) = 0.979). This grouping can be visualised more easily in the biplot shown in Fig. 3b, where the compounds closely associated with each sample were determined. Correlation scaling showed the metabolite variables associated with the Davidson plum and native currant samples had a greater significance to the a* and b* components than to L*. The L* was more significantly influenced by the metabolites which are also correlating to blueberry.

3.6. Correlation of metabolites to CIELAB

To investigate the effect that each compound has on colour for species, a PLS-DA model was generated using the CIELAB metrics (Table 1) and the pigments dataset (Table 3). The PLS-DA model explained 98.1 % of the variance across 2 components. PC1 explained 49.5 % while PC2 explained 48.6 %. The score plot of the PLS-DA (Fig. S1) had the same distinct grouping of the samples as the PLS model shown in Fig. 3. The coefficients of the major contributing metabolites (VIP > 1) are reported in Fig. 4. PLS-DA (Partial Least Squares Discriminant Analysis) coefficients elucidate the extent to which each metabolite influences the various colour metrics. In this context, L* measures lightness, a* measure the red/green value, and b* measure the yellow/blue value of the sample. These coefficients indicate the significance of each metabolite in determining these colour metrics. For instance, a metabolite with a high coefficient for L* strongly affects the lightness of the sample. Similarly,

high a* or b* coefficients suggest that the metabolite substantially influences the red/green or yellow/blue values, respectively. This analysis aids in identifying which metabolites are most crucial in influencing the colour characteristics of the sample. PLS-DA coefficients can be either positive or negative, reflecting the direction and magnitude of each metabolite impact on the colour metrics (L, a*, and b*). A positive coefficient implies that as the metabolite concentration increases, the colour metric value (i.e., L*, a*, or b*) also increases. For example, a positive coefficient for a* would indicate that higher levels of a particular metabolite are associated with a shift towards red in the colour spectrum. Conversely, a negative coefficient denotes that as the metabolite concentration increases, the value of the colour metric decreases. For instance, a negative coefficient for L* would indicate that higher levels of a specific metabolite result in a darker colour (lower lightness).

Anthocyanidin-3-O-glycosides and anthocyanidins emerged as the most influential metabolites for the a* metric, indicating their pivotal role in producing the red hues observed in Davidson plum and native currant. These findings are consistent with the literature where increased anthocyanin content is causative of fruit redness (Zhou et al., 2020). The elevated anthocyanin levels in the two Traditional fruits distinguished their pigmentation from the less intense red tones of the blueberry samples. Flavonoid glycosides contributed variably to the b* metric, reflecting their dual role in modulating yellow and blue hues depending on their structural properties and interactions with other pigments (Bartnik & Facey, 2024). Similarly, flavanols exhibited strong negative coefficients for L*, underscoring their impact on the darker tones in native currant, which had the lowest L* value among the samples. Flavanones, in contrast, demonstrated a positive influence on b*, supporting subtle yellow undertones. The reduced lightness (L*) and increased redness (a*) observed in native currant are attributed to its higher anthocyanidin content compared to Davidson plum and blueberry. Blueberry, in contrast, exhibited lighter tones influenced by metabolites such as biflavonoids, which contributed positively to L* and less intensely to a*. The unique separation of the fruit species within the PLS-DA space reflects their distinct metabolomic fingerprints. Native currant clustered distinctly due to its high anthocyanidin content and corresponding darker and redder pigmentation. Davidson plum displayed a similar but slightly lighter profile, while blueberry separated

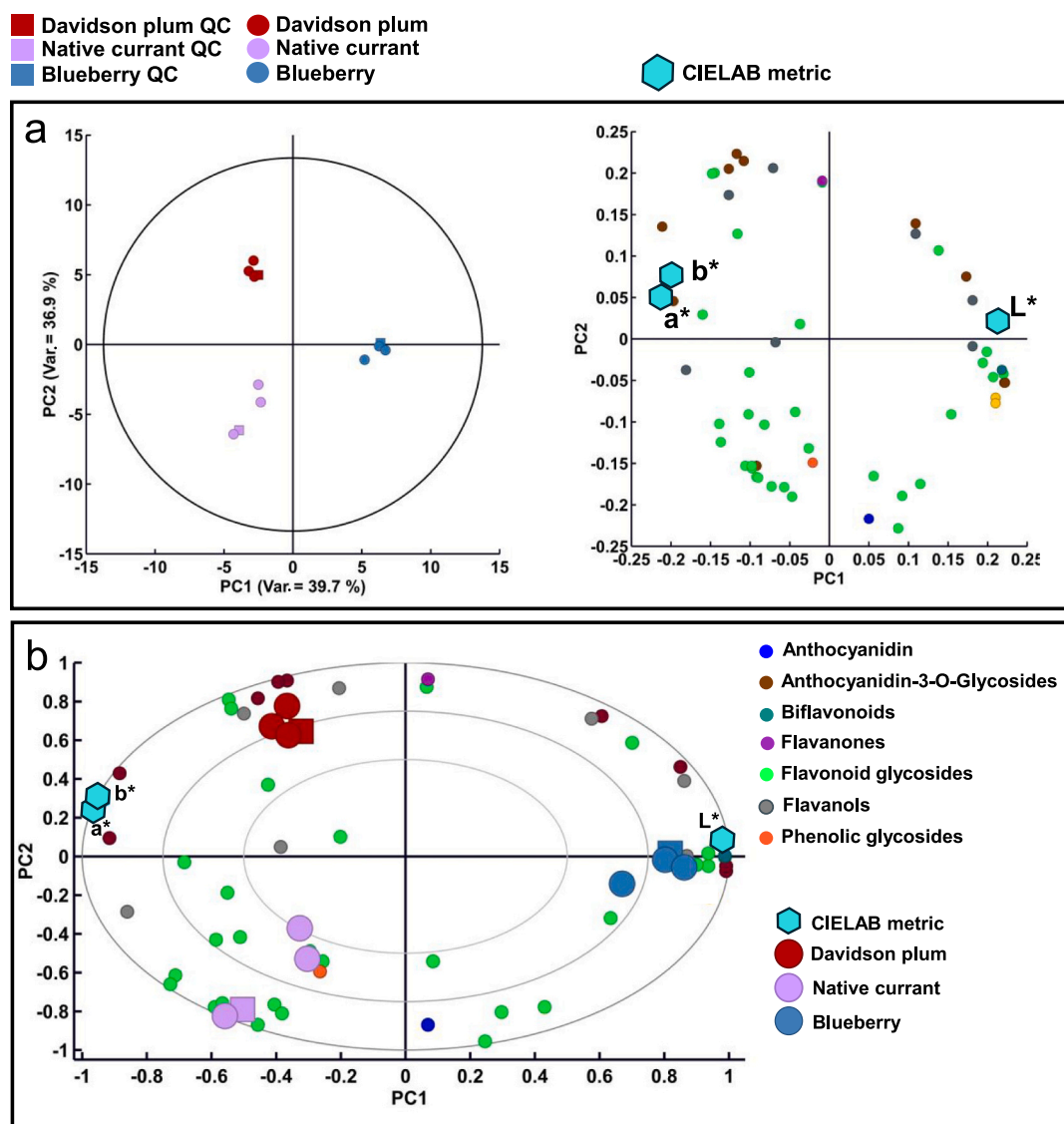


Fig. 3. Predictive multivariate analysis of CIELAB and pigment compounds in davidson plum, native currant, and blueberry. Fig. 3a: PLS scores and loadings plots of the pigment; R^2 (cum) = 76.7 % (PC1 = 39.7 %, PC2 = 36.9 %) Q^2 (cum) = 97.1 %. Fig. 3b: PLS biplot of pigment compounds and CIELAB colour metrics.

further due to its lower anthocyanidin levels and a more magenta-toned colour spectrum. These results highlight the significant role of anthocyanidins and their derivatives in driving the red hues of native currant and Davidson plum, with additional contributions from flavonoid glycosides and flavanols shaping their overall appearance. The findings further emphasise the potential of these native fruits as unique, high-intensity natural colourants suitable for a range of food applications.

3.7. UPLC-Q-ToF-MS-MS identification and reporting of selected pigmented compounds

In the present study, we adhere to the suggested guidelines for MS/MS data reporting to enable data transparency within the Australian Traditional food space which is still in its scientific infancy. In the positive ionisation, the protonated molecule ($[M + H]^+$) was determined by the initial identification in MS-DIAL, which gave the exact mass for potential molecular formula prediction. The position of sugar moieties was conducted by analysing the fragmentation patterns seen in the MS/MS spectra via neutral loss analysis (identification of specific neutral losses, such as the loss of a glucose moiety) and characteristic fragmentation of the sugar linkages based on collision-induced

dissociation. Where features containing common sugar masses were determined (such as in galactose and glucose), *In silico* identification was conducted in MS Finder, which gave the exact mass and compound identification as in MS Dial feature annotation. Herein, we acknowledge the limitations of *In silico* matching in that compound identification is inferior to the use of reference standards. *In silico* matching presents the best interpretation for the theoretical compound where similar sugar moieties are concerned. The native currant profile reported here is, to our knowledge, the first instance of metabolomic anthocyanin and flavonoid identification in *Antidesma erostre*. In summary, each species exhibited a unique anthocyanin composition which is in contrast to their visually similar colour. Furthermore, it is intriguing to note the compositional resemblance between Davidson plum and the native currant. Despite this similarity, the Davidson plum is characterised by a significant presence of delphinidin-3-O-sambubioside and cyanidin-3-O-sambubioside. Conversely, the native currant exhibits a high base delphinidin content while also having a broader spectrum of colour-contributing anthocyanins, underscoring a more diverse anthocyanin composition which indicates unique bioactivity as a functional food colouring. In literature, it is commonplace to report the phenolic content alongside colourimetry (Suriano et al., 2021; Trouillas et al., 2016).

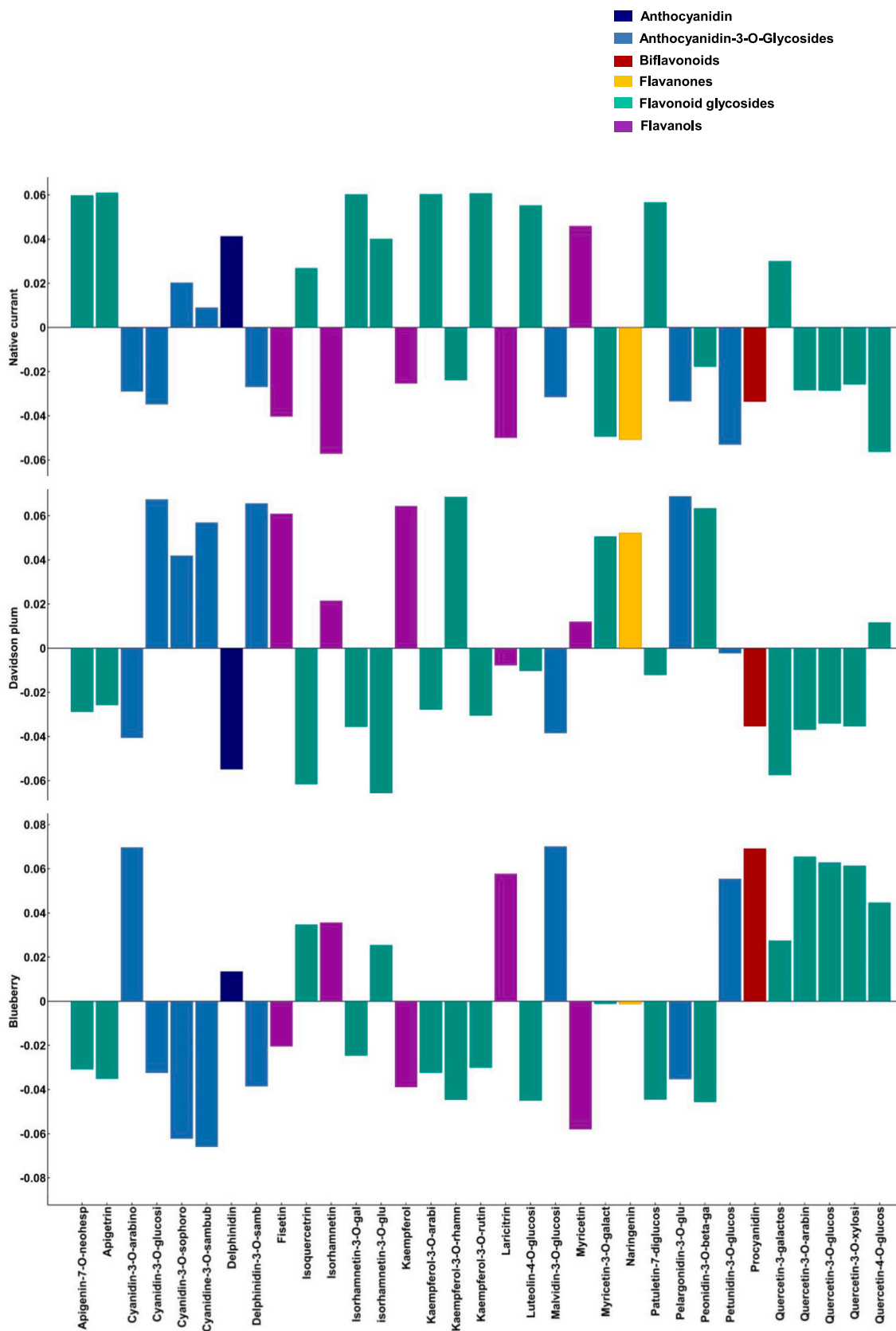


Fig. 4. Coefficient of metabolite contribution to CIELAB metric separation in native currant, davidson plum and blueberry. The positive coefficient means that as the metabolite concentration increases, the colour metric's value (L^* , a^* , or b^*) also increases. The positive coefficient for a^* indicates that higher levels of a particular metabolite are associated with a shift towards red in the colour spectrum. The negative coefficient means that as the metabolite concentration increases, the colour metric's value decreases. For example, a negative coefficient for L^* would indicate that higher levels of a specific metabolite result in a darker colour (lower lightness). (For interpretation of the references to colour in this figure legend, the reader is referred to the web version of this article.)

However, there is a lack of metabolomic workflows that aim to delineate between specific anthocyanins and their contribution to a CIELAB measurement.

The chemical stability of the pigment extracts from Davidson plum and native currant is a critical factor that influences their viability as natural food colourants. While the present study highlighted their vibrant pigmentation and bioactive potential, the stability of these pigments under various environmental conditions, such as changes in pH, temperature, and light exposure, remains an area requiring further exploration. Stability is particularly important for ensuring consistency and durability in industrial applications, where pigments must retain their colour and bioactivity during processing and storage. Given the importance of these factors, a follow-up study focusing on the chemical stability of Traditional food extracts is warranted. Such a study would provide valuable insights into the mechanisms of pigment degradation, strategies for stabilisation, and practical guidelines for incorporating the pigments into commercial food products, thereby advancing their utility in the food industry.

4. Conclusions

This study showcases the potential of two Australian native foods through a comprehensive analysis involving visual inspection, colourimetry, and quantitative assessment of metabolites. Furthermore, we have presented a workflow for the nomination of discernible metabolites that drive fruit colouring by employing a stepwise multivariate approach that utilised UPLC-Q-ToF-MS/MS. The major outcome of this is the support of native currant and Davidson plum for use as natural food colourants and a nutraceutical ingredient. Further exploration into the composition and applications of *Antidesma erosre* is warranted, offering new avenues for both food research and the emerging 'bushfood' industry. This study also underscored the significant value to be found in Tradition foods for diversifying the global food market. By leveraging advanced analytical techniques, including CIELAB colourimetry and high-resolution mass spectrometry, the unique colour profiles and potential applications of these native species have been elucidated. Moreover, the identification of specific metabolites responsible for their colouration opens doors for targeted utilisation and further exploration of their nutritional and functional properties. This research contributes to the broader understanding of Indigenous food sources and fosters sustainable practices in the food additives industry.

Funding

This study is funded by the Australian Research Council 20/21 Discovery grant: 'A Deadly Solution: Towards an Indigenous-led bush food industry'. GA ID: GA141113.

CRediT authorship contribution statement

Thomas Owen Hay: Writing – review & editing, Writing – original draft, Visualization, Validation, Methodology, Investigation, Formal analysis, Data curation, Conceptualization. **Melissa A. Fitzgerald:** Writing – review & editing, Supervision, Funding acquisition. **Joseph Robert Nastasi:** Writing – review & editing, Visualization, Supervision, Methodology, Formal analysis.

Declaration of competing interest

The authors declare no conflict of interest. The funders had no role in the design of the study; in the collection, analyses, or interpretation of data; in the writing of the manuscript, or in the decision to publish the results.

Acknowledgments

The Authors acknowledge the Traditional Owners of these species, and the lands on which we work, the many First Nations peoples of Australia. We are truly grateful to work in partnership in such endeavours and pay our respects to Elders of past and present. Specifically, we would like to thank Gerry Turpin, Cherry Turpin, Valmai Turpin, Suzanne Thompson, Dale Chapman, and Bronwyn Fredericks for informing and guiding us in Traditional Knowledge and their guidance when sourcing and investigating Australian genetic resources.

Appendix A. Supplementary data

Supplementary data to this article can be found online at <https://doi.org/10.1016/j.fochx.2024.102072>.

Data availability

Data is not publicly available due to a non-disclosure agreement with Traditional Owners.

References

- Ahmed, M. A., Al-Khalifa, A. S., Al-Nouri, D. M., & El-Din, M. F. S. (2021). Dietary intake of artificial food color additives containing food products by school-going children. *Saudi Journal of Biological Sciences*, 28(1), 27–34.
- Aleekh, S., Aharoni, A., Brotman, Y., Contrepoint, K., D'Auria, J., Ewald, J., ... Fernie, A. R. (2021). Mass spectrometry-based metabolomics: A guide for annotation, quantification and best reporting practices [article]. *Nature Methods*, 18(7), 747–756. <https://doi.org/10.1038/s41592-021-01197-1>
- de Araújo, F. F., de Paulo Farias, D., Neri-Numa, I. A., & Pastore, G. M. (2021). Polyphenols and their applications: An approach in food chemistry and innovation potential. *Food Chemistry*, 338, Article 127535. <https://doi.org/10.1016/j.foodchem.2020.127535>
- Bartnik, M., & Facey, P. (2024). Glycosides. In *Pharmacognosy* (pp. 103–165). Academic Press.
- Batiha, G. E.-S., Hussein, D. E., Algammal, A. M., George, T. T., Jeandet, P., Al-Snafi, A. E., ... Thorat, N. D. (2021). Application of natural antimicrobials in food preservation: Recent views. *Food Control*, 126, Article 108066.
- Bora, P., Das, P., Bhattacharyya, R., & Barooah, M. S. (2019). Biocolour: The natural way of colouring food. *Journal of Pharmacognosy and Phytochemistry*, 8(3), 3663–3668.
- Caldeira, I., Lopes, D., Delgado, T., Canas, S., & Anjos, O. (2018). Development of blueberry liquor: Influence of distillate, sweetener and fruit quantity. *Journal of the Science of Food and Agriculture*, 98(3), 1088–1094.
- Cesa, S., Carradori, S., Bellagamba, G., Locatelli, M., Casadei, M. A., Masci, A., & Paolicelli, P. (2017). Evaluation of processing effects on anthocyanin content and colour modifications of blueberry (*Vaccinium* spp.) extracts: Comparison between HPLC-DAD and CIELAB analyses. *Food Chemistry*, 232, 114–123.
- Chuen, T. L. K., Vuong, Q. V., Hirun, S., Bowyer, M. C., Predebon, M. J., Goldsmith, C. D., ... Scarlett, C. J. (2016). Antioxidant and anti-proliferative properties of davidson's plum (*Davidsonia pruriens* F. Muell) phenolic-enriched extracts as affected by different extraction solvents. *Journal of Herbal Medicine*, 6(4), 187–192. <https://doi.org/10.1016/j.hermed.2016.08.005>
- Darniadi, S., Ho, P., & Murray, B. S. (2018). Comparison of blueberry powder produced via foam-mat freeze-drying versus spray-drying: Evaluation of foam and powder properties. *Journal of the Science of Food and Agriculture*, 98(5), 2002–2010. <https://doi.org/10.1002/jsfa.8685>
- Dechayont, B., Itharat, A., Phuaklee, P., Chunthorn-Orn, J., Juckmeta, T., Prommee, N., Nuengchamnong, N., & Hansakul, P. (2017). Antioxidant activities and phytochemical constituents of *antidesma thwaitesianum* Müll. Arg. leaf extracts. *Journal of Integrative Medicine*, 15(4), 310–319.
- Deledda, A., Annunziata, G., Tenore, G. C., Palmas, V., Manzin, A., & Velluzzi, F. (2021). Diet-derived antioxidants and their role in inflammation, obesity and gut microbiota modulation. *Antioxidants*, 10(5), 708.
- Ding, N., Zhou, Y., Dou, P., Chang, S. K., Feng, R., Hong, H., ... Tan, Y. (2024). Colorful and nutritious abundance: Potential of natural pigment application in aquatic products. *Food Innovation and Advances*, 3(3), 232–243.
- Echegaray, N., Guzel, N., Kumar, M., Guzel, M., Hassoun, A., & Lorenzo, J. M. (2023). Recent advancements in natural colorants and their application as coloring in food and in intelligent food packaging. *Food Chemistry*, 404, Article 134453.
- Escher, G. B., Wen, M., Zhang, L., Rosso, N. D., & Granato, D. (2020). Phenolic composition by UHPLC-Q-TOF-MS/MS and stability of anthocyanins from *Clitoria ternatea* L. (butterfly pea) blue petals. *Food Chemistry*, 331, Article 127341.
- Faria, A., Oliveira, J., Neves, P., Gameiro, P., Santos-Buelga, C., de Freitas, V., & Mateus, N. (2005). Antioxidant properties of prepared blueberry (*Vaccinium myrtillus*) extracts. *Journal of Agricultural and Food Chemistry*, 53(17), 6896–6902.
- Gantenbein, K. V., & Kanaka-Gantenbein, C. (2021). Mediterranean diet as an antioxidant: The impact on metabolic health and overall wellbeing. *Nutrients*, 13(6), 1951.

- Hay, T., Prakash, S., Daygon, V. D., & Fitzgerald, M. (2022). Review of edible Australian flora for colour and flavour additives: Appraisal of suitability and ethicality for bushfoods as natural additives to facilitate new industry growth. *Trends in Food Science & Technology*, *123*, 1–14.
- Krongyut, O., & Sutthanut, K. (2019). Phenolic profile, antioxidant activity, and anti-obesogenic bioactivity of Mao Luang fruits (*Antidesma bunius* L.). *Molecules*, *24*(22), 4109.
- Lee, J., Durst, R. W., Wrolstad, R. E., Kupina, C. E. T. G. M. H. J. H. H. K. S. K. D., & JD, S. M. S. M. B. M. T. P. F. R. A. S. G. T. U. W. (2005). Determination of total monomeric anthocyanin pigment content of fruit juices, beverages, natural colorants, and wines by the pH differential method: Collaborative study. *Journal of AOAC International*, *88*(5), 1269–1278.
- Li, X., Zhu, F., & Zeng, Z. (2021). Effects of different extraction methods on antioxidant properties of blueberry anthocyanins. *Open Chemistry*, *19*(1), 138–148.
- Lim, V., Gorji, S. G., Daygon, V. D., & Fitzgerald, M. (2020). Untargeted and targeted metabolomic profiling of Australian indigenous fruits. *Metabolites*, *10*(3), 114. <https://doi.org/10.3390/metabo10030114>
- di Lorenzo, C., Colombo, F., Biella, S., Stockley, C., & Restani, P. (2021). Polyphenols and human health: The role of bioavailability. *Nutrients*, *13*(1), 273.
- Luo, M. R. (2023). Cielab. In *Encyclopedia of color science and technology* (pp. 251–257). Springer.
- Lyu, X., Lyu, Y., Yu, H., Chen, W., Ye, L., & Yang, R. (2022). Biotechnological advances for improving natural pigment production: A state-of-the-art review. *Bioresources and Bioprocessing*, *9*(1), 8.
- Mani, J. S., Johnson, J. B., Hosking, H., Ashwath, N., Walsh, K. B., Neilsen, P. M., ... Naiker, M. (2020). Antioxidative and therapeutic potential of selected Australian plants: A review. *Journal of Ethnopharmacology*, *268*(2021), 113580.
- Manzoor, M., Singh, J., Gani, A., & Noor, N. (2021). Valorization of natural colors as health-promoting bioactive compounds: Phytochemical profile, extraction techniques, and pharmacological perspectives. *Food Chemistry*, *362*, Article 130141.
- Mudgal, D., Singh, S., & Singh, B. R. (2022). Nutritional composition and value added products of beetroot: A review. *Journal of Current Research in Food Science*, *3*(1), 01–09.
- Nastasi, J. R., Daygon, V. D., Kontogiorgos, V., & Fitzgerald, M. A. (2023). Qualitative analysis of polyphenols in glycerol plant extracts using untargeted metabolomics. *Metabolites*, *13*(4), 566.
- Nastasi, J. R., Fitzgerald, M. A., & Kontogiorgos, V. (2023). Tuning the mechanical properties of pectin films with polyphenol-rich plant extracts. *International Journal of Biological Macromolecules*, *253*, Article 127536.
- Nirmal, N. P., Mereddy, R., Webber, D., & Sultanbawa, Y. (2021). Biochemical, antioxidant and sensory evaluation of davidsonia pruriens and davidsoina jerseyana fruit infusion. *Food Chemistry*, *342*, Article 128349.
- Njume, C., McAinch, A. J., & Donkor, O. (2020). Proximate and phenolic composition of selected native Australian food plants. *International Journal of Food Science & Technology*, *55*(5), 2060–2079.
- Nwoba, E. G., Ogbonna, C. N., Ishika, T., & Vadiveloo, A. (2020). Microalgal pigments: A source of natural food colors. *Microalgae Biotechnology for Food, Health and High Value Products*, 81–123.
- Papas, A. M. (2019). *Antioxidant status, diet, nutrition, and health*. CRC Press.
- Puangpoy, P., Kittipongpittaya, K., Khoontawad, J., Jorjong, S., Phalangsuk, N., Phansuwan, T., Senggam, P., Boonpui, O., Lertsit, K., & Sooksabine, K. (2024). Phytochemical screening, total phenolics, total flavonoids, total tannins, antioxidant activities, and α -glucosidase inhibition of ethanolic leaf extracts from 37 cultivars of *Antidesma punctulatum* Miq. *Journal of Hermed Pharmacology*, *13*(1), 61–73.
- Rana, A., Samtiya, M., Dhewa, T., Mishra, V., & Aluko, R. E. (2022). Health benefits of polyphenols: A concise review. *Journal of Food Biochemistry*, *46*(10), Article e14264.
- Redondo-Blanco, S., Fernández, J., López-Ibáñez, S., Miguélez, E. M., Villar, C. J., & Lombó, F. (2020). Plant phytochemicals in food preservation: Antifungal bioactivity: A review. *Journal of Food Protection*, *83*(1), 163–171. <https://doi.org/10.4315/0362-028X.JFP-19-163>
- da Rosa, J. R., Nunes, G. L., Motta, M. H., Fortes, J. P., Weis, G. C. C., Hecktheuer, L. H. R., ... da Rosa, C. S. (2019). Microencapsulation of anthocyanin compounds extracted from blueberry (*Vaccinium* spp.) by spray drying: Characterization, stability and simulated gastrointestinal conditions. *Food Hydrocolloids*, *89*, 742–748.
- Sánchez-Rangel, J. C., Benavides, J., Heredia, J. B., Cisneros-Zevallos, L., & Jacobo-Velázquez, D. A. (2013). The folin-ciocalteu assay revisited: improvement of its specificity for total phenolic content determination. *Analytical Methods*, *5*(21), 5990–5999.
- Spence, C., Motoki, K., & Petit, O. (2022). Factors influencing the visual deliciousness/eye-appeal of food. *Food Quality and Preference*, *102*, Article 104672.
- Suriano, S., Balconi, C., Valoti, P., & Redaelli, R. (2021). Comparison of total polyphenols, profile anthocyanins, color analysis, carotenoids and tocopherols in pigmented maize. *LWT*, *144*, Article 111257.
- Tan, A. C., Koneczak, I., Ramzan, I., & Sze, D. M.-Y. (2011). Antioxidant and cytoprotective activities of native Australian fruit polyphenols. *Food Research International*, *44*(7), 2034–2040.
- Trouillas, P., Sancho-García, J. C., de Freitas, V., Gierschner, J., Otyepka, M., & Dangles, O. (2016). Stabilizing and modulating color by copigmentation: Insights from theory and experiment. *Chemical Reviews*, *116*(9), 4937–4982.
- Yan, Y., Pico, J., Gerbrandt, E. M., Dossett, M., & Castellari, S. D. (2023). Comprehensive anthocyanin and flavonol profiling and fruit surface color of 20 blueberry genotypes during postharvest storage. *Postharvest Biology and Technology*, *199*, Article 112274.
- Yang, W., Guo, Y., Liu, M., Chen, X., Xiao, X., Wang, S., ... Chen, F. (2022). Structure and function of blueberry anthocyanins: A review of recent advances. *Journal of Functional Foods*, *88*, Article 104864.
- Zanoni, F., Primiterra, M., Angeli, N., & Zoccatelli, G. (2020). Microencapsulation by spray-drying of polyphenols extracted from red chicory and red cabbage: Effects on stability and color properties. *Food Chemistry*, *307*, Article 125535.
- Zhou, Y., Gao, Y. G., & Giusti, M. M. (2020). Accumulation of anthocyanins and other phytochemicals in American elderberry cultivars during fruit ripening and its impact on color expression. *Plants*, *9*(12), 1721.